

Effect of Adding Porous Strips to Centrifugal Compressor Blades on its Flow Instabilities

Tamer S. Fathy¹, Aly Elzahaby², Mohamed K. Khalil³, and N. Elquassas⁴

Abstract: This paper discusses the effect of adding porous strips to the centrifugal compressor blades on its flow instabilities by eliminating the rotating stall phenomena and then extending the compressor operating range. Porous strips are added on the suction side of the impeller main blades, on certain predetermined locations in previous work [1].

a parametric study on the effect of adding porous media on the flow instabilities in the centrifugal compressor will be discussed. The porous media has been familiarized on the compressor impeller. Simulations, at a flow rate near the stall point mass flow rate as predicted by the test map have been investigated in order to study the effect of adding porous media on the flow behavior. Initially, the study analyzes the effect of the predefined porous media applied to the impeller domain. Finally, localized porous strips have been modeled on the impeller blade to study their effects on the flow field.

The centrifugal compressor model used in this study as a reference to be compared with the obtained porous results was conducted for JetCat P200-SX. The JetCat P200-SX turbojet engine complete technical specifications are given in Table 1.

Table-1: JETCAT P200sx Technical Specifications as Provided from Manufacture

Compressor pressure ratio, π_{ct}	3.7
Idle thrust N	9 N
Maximum Thrust, N	230 N
Idle Speed	33,000 rpm
Maximum Speed	112,000 rpm
Maximum Exhaust Gas Temperature (EGT)	750°C
Mass Flow Rate, \dot{m}	0.45 kg/s
Maximum exhaust velocity	1,840 km/hr
Maximum fuel consumption	0.584 kg/min (0.1523 kgf/Nh)
Fuel mixture (By volume)	95% Jet-A1+ 5% Mobil jet oil
	254

ANSYS CFX-17.2 solver is employed to analyze the performance and the internal flow of the centrifugal compressor with four different strip configurations on the suction side of the impeller main blade. The porous material is suggested with hope to obtain the larger stall margin and the higher efficiency. In practical the porous ceramic coating can be developed using plasma spraying process.

Index Terms—: compressor map, stall margin, porous strip, CFX.

1. Introduction

The operating range in centrifugal compressors is limited at low mass flow rate by the rotating stall phenomena and at a high mass flow rate by choke. The rotating stall is a potential threat to the compression system because a stall cell generates excessive vibrations and stresses on the compressor blade and may lead to its structural failure. Avoiding the phenomena of rotating stall is one of the most important issues for compressor designers. The porous material is suggested to be used here as the porous media suppresses the growth of the flow boundary layer [2], which gives the compressor larger stall margin [3]. In practical the porous ceramic coating can be developed using plasma spraying process. The mixture of 8 wt. % yttria-stabilized zirconia and polyester powders can be used as the coating material. A simulation test of gas flow around the gas turbine blade verified a remarkable reduction of the coating surface temperature by the transpiration cooling mechanism. It was concluded that the transpiration cooling system for the gas turbine could be achieved using the developed porous ceramic coating [4].

An attempt has been made to reduce the compressor instability and subsequently increase the surge margin by the application of adding porous strips on different parts of the impeller blade. To start the evaluation, it is important to study the effect of the porous strip's location on the flow structure within the centrifugal compressor. Ansys CFX-17.2 has been employed to calculate the flow field in the centrifugal compressor. The porous strips are defined in the solver as sub-domains of the rotating impeller domain. The sub-domain allows sources of energy, mass, momentum, radiation, components and turbulence to be specified. When modeling porous momentum losses, a momentum loss due to an obstruction in the flow direction, such as honeycombs, porous filters and soon, the isotropic and directional loss models are useful. The porous strips are defined as an isotropic loss model which has a permeability of $8.53 \times 10^{-10} \text{ m}^2$ and an inertial resistance factor of 13.672 m^{-1} . The pressure distribution on the suction side of the impeller blade at $\bar{n} = 0.73$ for a stable point near stall can be shown in Figure 1.

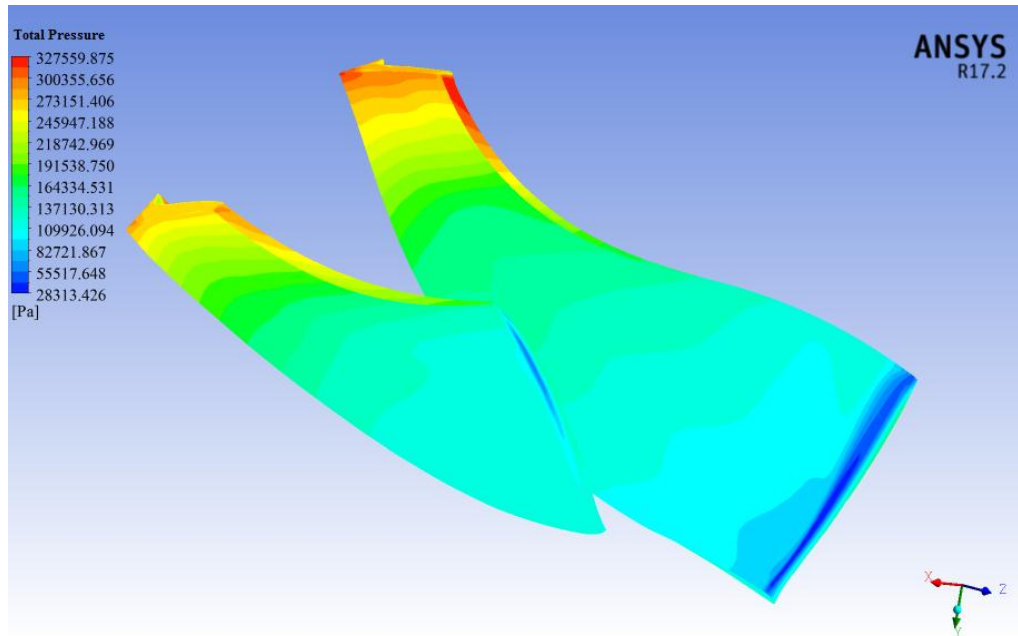


Fig.1: Total pressure contours on blade suction side at $\bar{n} = 0.73$ near stall

The distribution of total pressure gives an indication of the flow disturbances and losses. Thus, the regions with a lower value of the total pressure correspond to the locations where the generated losses are significantly greater. According to the last figure four sub-regions on the suction surface of the impeller blade has been created. The four strips on the impeller blade have been referred to as "01", "02", "03" and "04". The study has been carried out by CFX-17.2 simulation at an outlet total pressure corresponding to the last stable operating point defined by the compressor map evaluated in the previous chapter using three cases of study (at $\bar{n} = 0.73$, $\bar{n} = 0.85$ and at design speed). The smooth baseline case forms the benchmark for the current analysis, so in order to conduct a comparative study, all the results have been compared with the smooth case. Figure 2 shows the modified impeller domains for the parametric porous study.

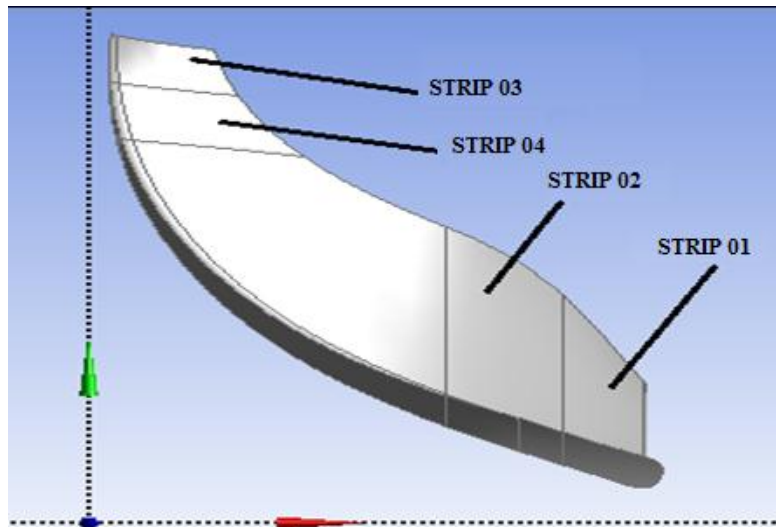


Fig.2: Modified impeller domains for the parametric porous study

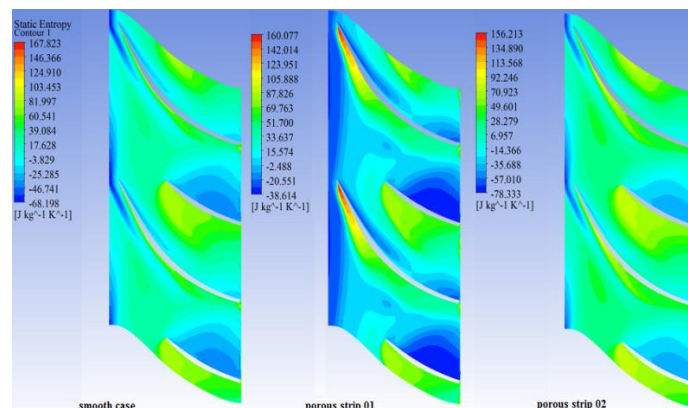
Table 2 represents the performance characteristics of CFX compressor model at the stable point near stall for $\bar{n} = 0.73$.

Table-2: Performance characteristics of CFX compressor model at

State	\dot{m} [kg/s]	π_{ct}	η_{ct}	Total Pressure at compressor outlet [Pa]	Velocity at compressor outlet [m/s]	Mach no. at compressor outlet [m/s]
Smooth case	0.2799	2.373	78.74	237944	110.716	0.282072
Porous strip 01	0.29	2.399	77.07	239485	117.069	0.298167
Porous strip 02	0.2795	2.374	78.72	238010	111.208	0.28332
Porous strip 03	0.2825	2.387	77.08	237616	109.531	0.279052
Porous strip 04	0.2819	2.387	77.03	237556	109.357	0.278594

2. Effect of porous strips on the impeller flow field

This section presents the effect of adding porous strips on the flow field of the centrifugal impeller. The impeller flow nature at the exit flow has a high effect on the compressor stage performance [3]. Thus, an investigation has been performed in details to study the effect of porous strips on the flow structure in the impeller. Since the stall and surge are unsteady phenomena so it is difficult to analyze the improvement in the flow structure using steady-state simulations. Nevertheless, a brief understanding has been discussed by considering the behavior of flow at different locations in the impeller domain.



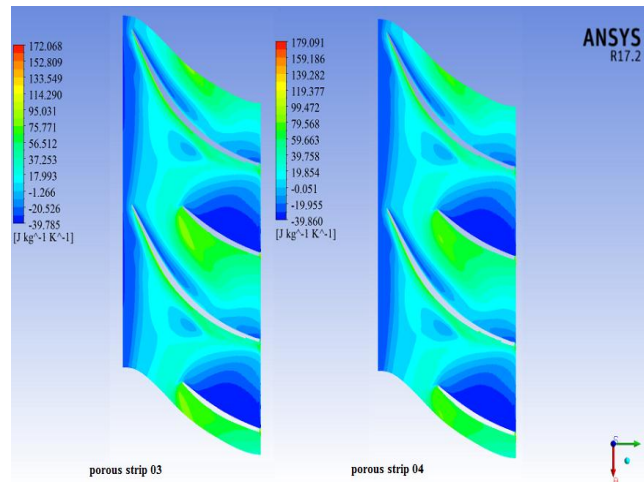
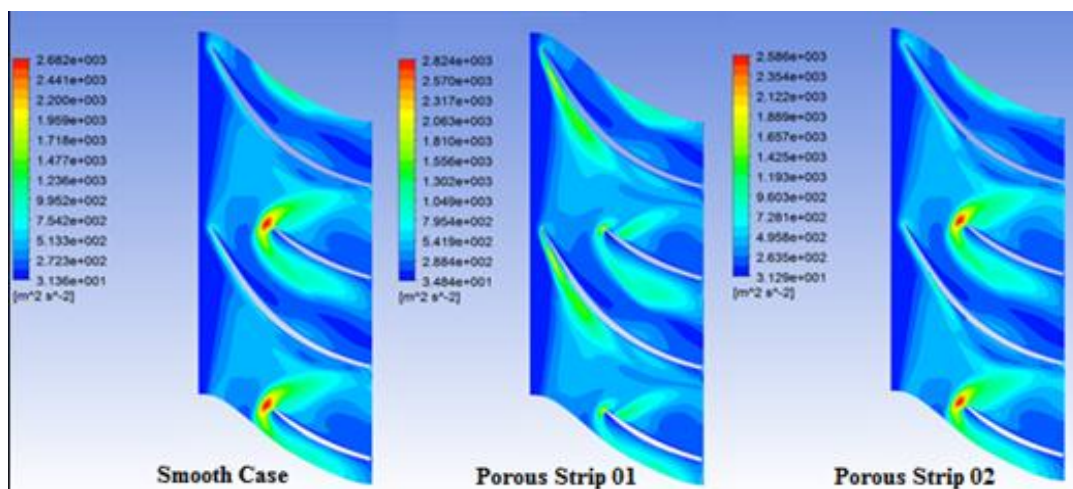


Fig.3: Static entropy contours on a section located at 99 % of the impeller and diffuser spanwise direction

The rise of entropy is strictly linked to the loss of total pressure and the efficiency of the radial flow compressor. Figure 3 shows the entropy distribution at a section located at 99 % of the impeller and diffuser spanwise direction. Low-entropy regions are generated in porous strip cases 01, 03 and 04 due to an increase in total pressure, in comparison to the reference case. The entropy distribution in porous strip case 02 is not in a far way different when compared with the reference smooth case.

Figure 4 shows that the adding of porous strip 01, 03 and 04 on the suction side of an impeller blade causes an increase in the turbulent kinetic energy and thus improves the stability of the flow. While the adding of porous strip 02 causes the turbulent kinetic energy to be decreased. The strong vortex generated due to adding porous strip increases the turbulent kinetic energy of the internal flow, which is favorable to extend the stable operating range. Porous strips 0.1, 0.3 and 04 increases the turbulent kinetic energy generated by the vortex and hence has a contribution to the stall margin improvement.



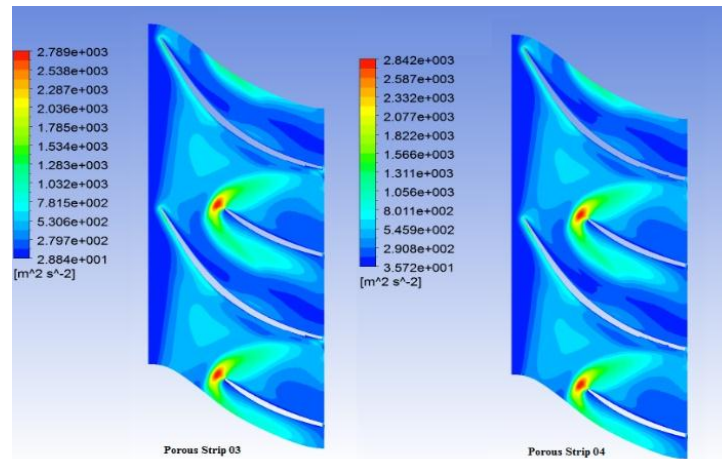
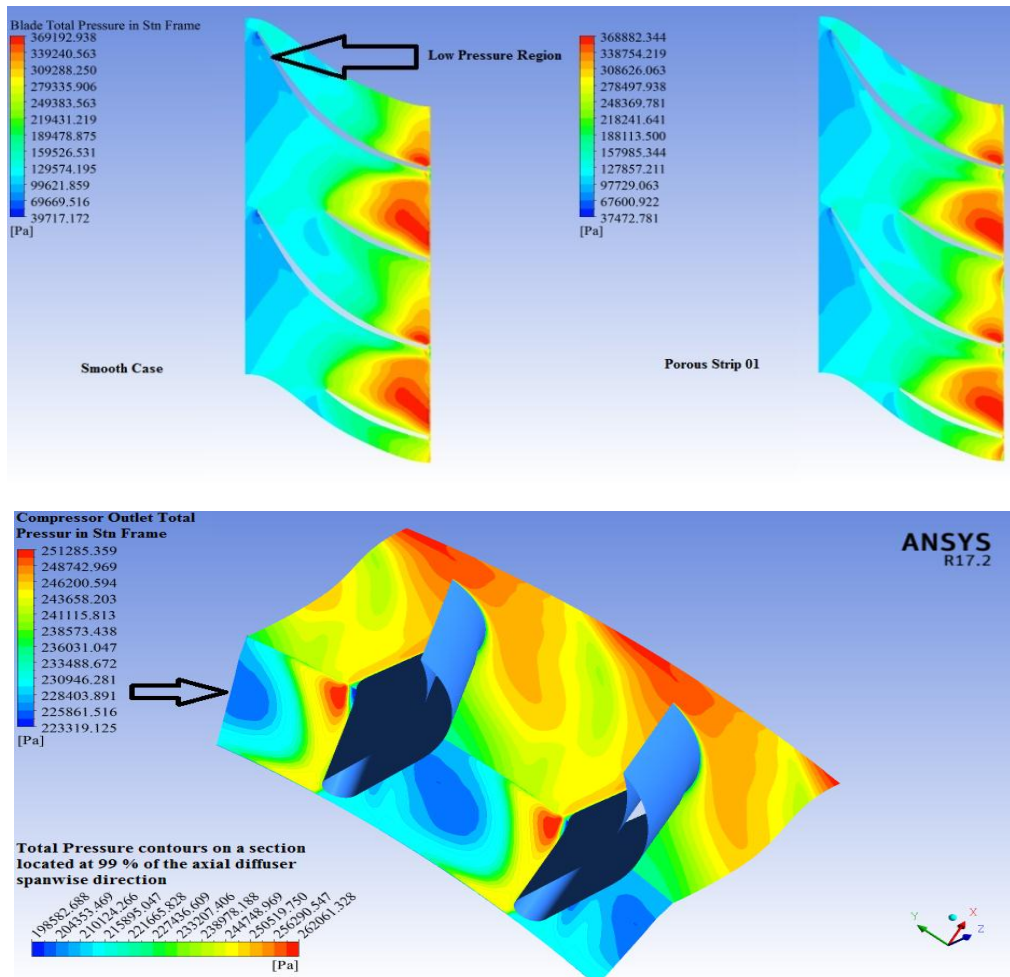


Fig.4: Turbulence K.E contours on a section located at 99 % of the impeller and diffuser spanwise direction

2.1 Porous strip 01

Figure 5 shows the contours of the total pressure of the impeller main blade and the axial diffuser at a section located at 99 % of spanwise direction for $\bar{n} = 0.73$.



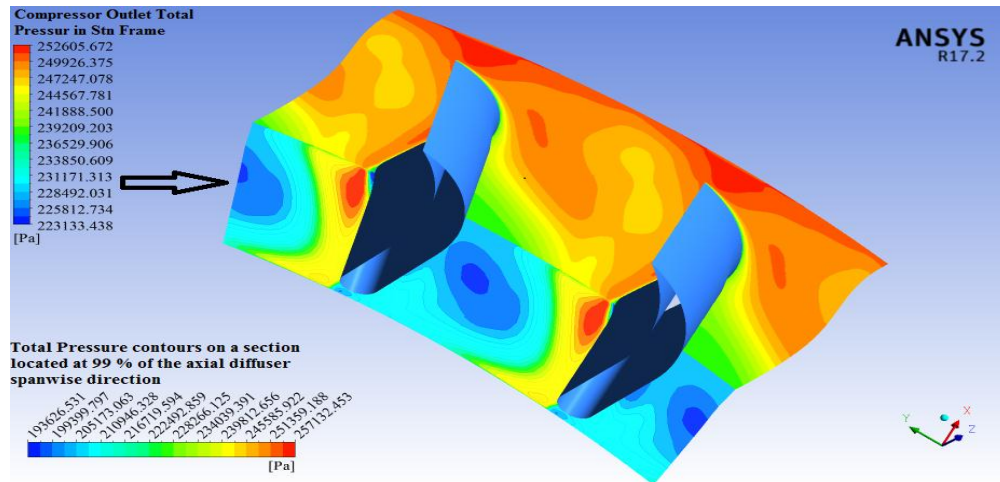


Fig.5: Total pressure contours on a section located at 99 % of the impeller and diffuser spanwise direction for the smooth case and porous strip 01

In the smooth case shown on the left side of Figure 5, it can be observed that close to the main blade’s suction side, an area of low total pressure is present (depicted by the blue region). This region can be attributed to the wake that develops as a result of the three-dimensional separation due to the secondary flows. Adding porous strip 01 close to the leading edge of the impeller blade causes a buildup in mass flow rate (when compared with the smooth case) and as a result a more stable operation of the compressor is observed as shown in the right side of Figure 5 causing a reduction of the low total pressure region at the impeller blade suction side, also a pressure buildup can be noticed at the compressor outlet (depicted in the axial diffuser region) [5].

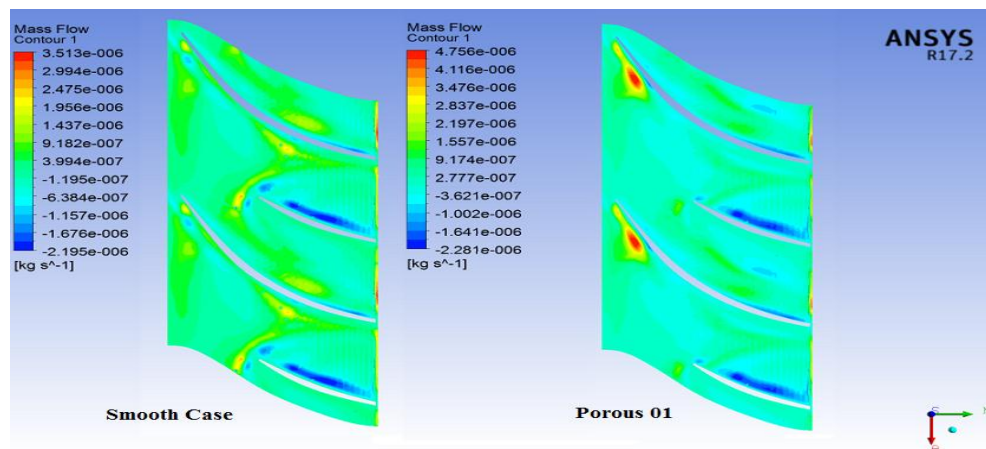


Fig.6: Mass flow contours on a section located at 99 % of the impeller and diffuser spanwise direction for smooth case and porous strip 01

It can be shown from Figure 6 that adding localized porous strip close to the blades leading causes a significant increase in mass distribution close to the trailing edge. The effective gain over the porous case can be attributed to the reduced blockage accounted for the boundary layer thickness and reduction in the separated flow region. Thus, the localized porous strip presents itself as an improvement over the smooth case. Figure 7 & Figure 8 present the velocity contours on a section located at 99 % of the impeller and diffuser spanwise direction for both smooth case and porous 01 respectively. The contour plots reveal a reduction in the wake region at the blade trailing edge and an improvement in the compressor outlet flow speed. This explains the gain in the mass flow observed in Figure 6.

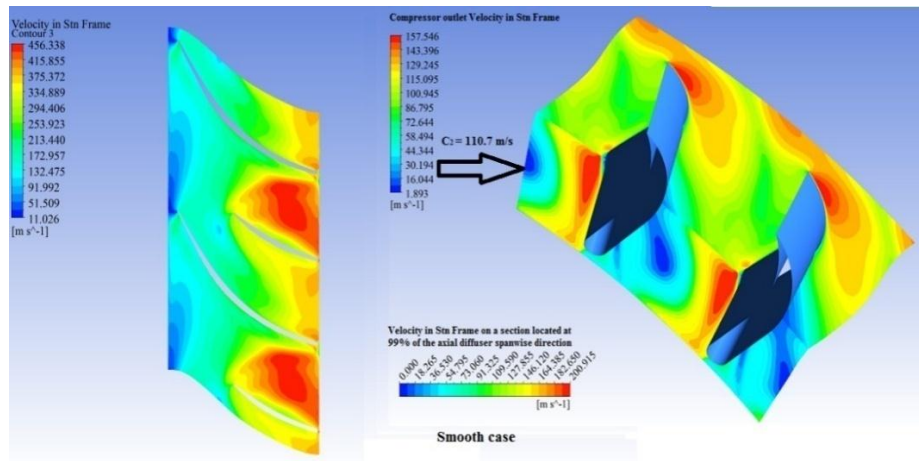


Fig.7: Velocity contours on a section located at 99 % of the impeller and diffuser spanwise direction for the smooth case

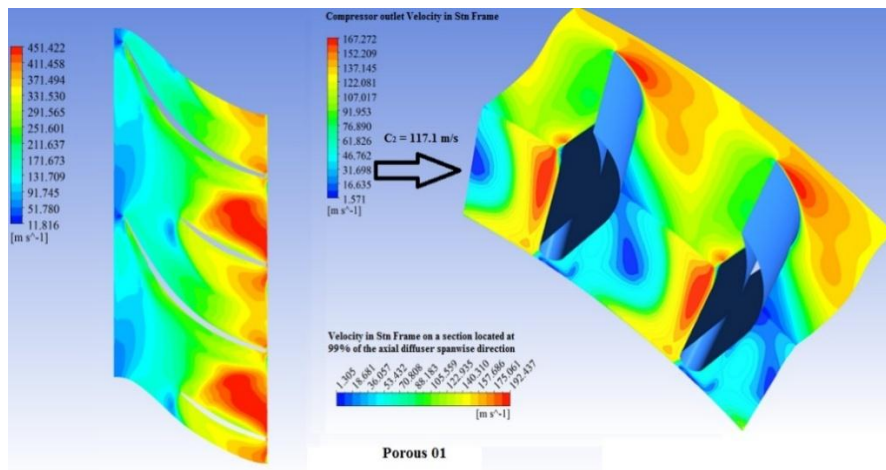


Fig.8: Velocity contours on a section located at 99 % of the impeller and diffuser spanwise direction for porous strip 01

2.2 Porous strip 02

Figure 9 presents the effect of porous strip 02 in terms of variation of the total pressure at the blade’s suction surface. It is evident from the contours depicted that there is no big change in the limitation of the wake region of the total pressure due to adding the porous strip 02 when compared with the smooth case.

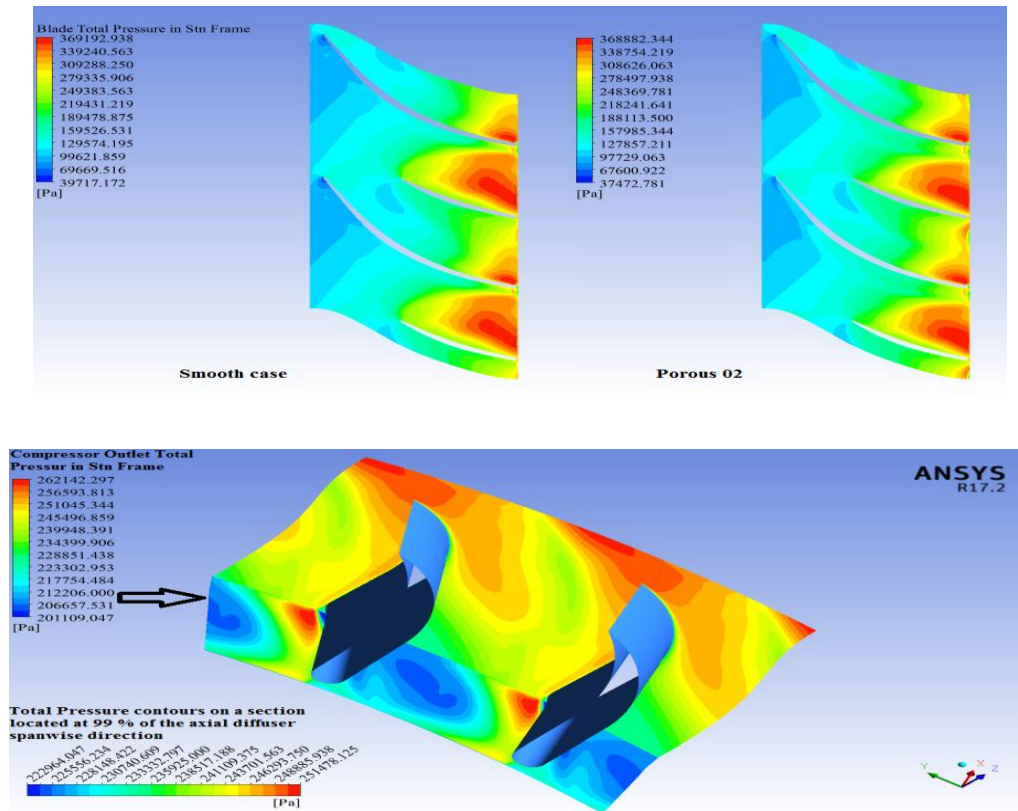


Fig.9: Total pressure contours on a section located at 99 % of the impeller and diffuser spanwise direction for the smooth case and porous strip 02

However, in comparison to the mass flux gain achieved by adding porous strip 02 as in Figure 10, it can be noticed that an increase in the mass flux distribution at the trailing edge of the impeller blade is generated due to the porous strip 02. This increase in the mass flux signifies a reduction in the trailing edge low momentum flow region. Comparing this gained mass flux with the one achieved by adding porous strip 01 leads to that the gain achieved in this case is lower.

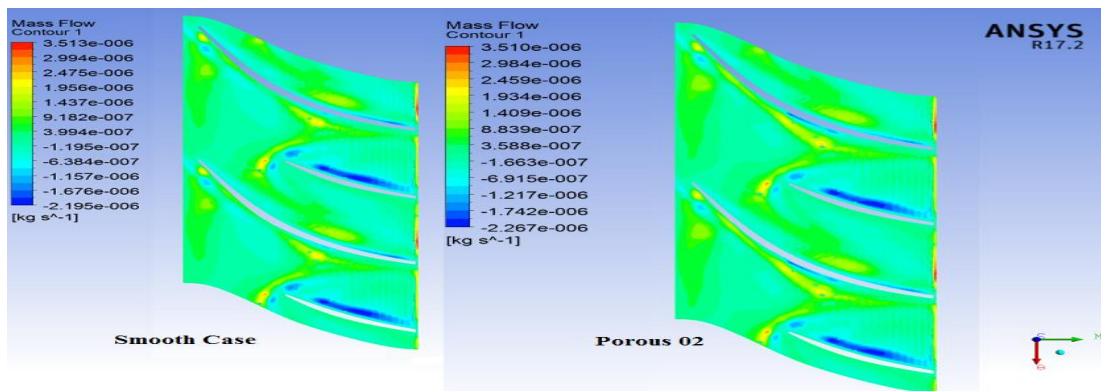


Fig.10: Mass Flow contours on a section located at 99 % of the impeller and diffuser spanwise direction for the smooth case and porous strip 02

Additionally, the velocity distribution at a spanwise direction on a section located at 99 % of the impeller and diffuser is depicted in the contour plots in Figure 11. The addition of the porous strip 02 causes a reduction in the low momentum wake region. However, the gain observed in this case is lower than the case in which strip 01 is introduced.

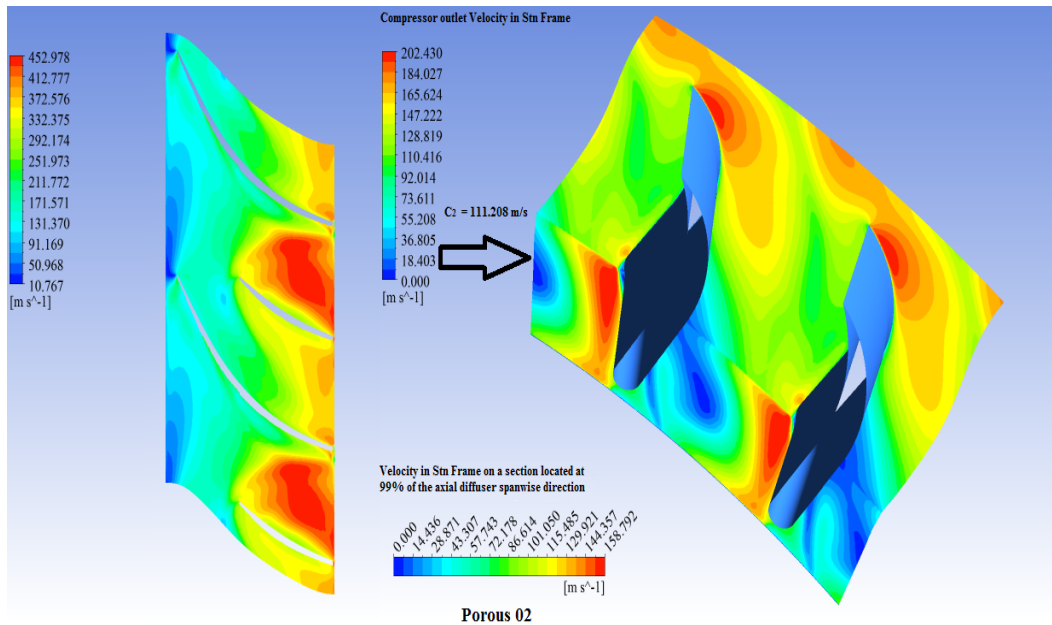


Fig.11: Velocity contours on a section located at 99 % of the impeller and diffuser spanwise direction for porous strip 02

2.3 Porous strip 03

Figure 12 illustrates the effect of adding localized porous strip 03 on the flow field of the impeller. It can be inferred that adding porous strip 03 to the impeller results in reducing the distribution of the mass flow at the impeller in comparison with the porous strip 01 and strip 02 in the impeller domain.

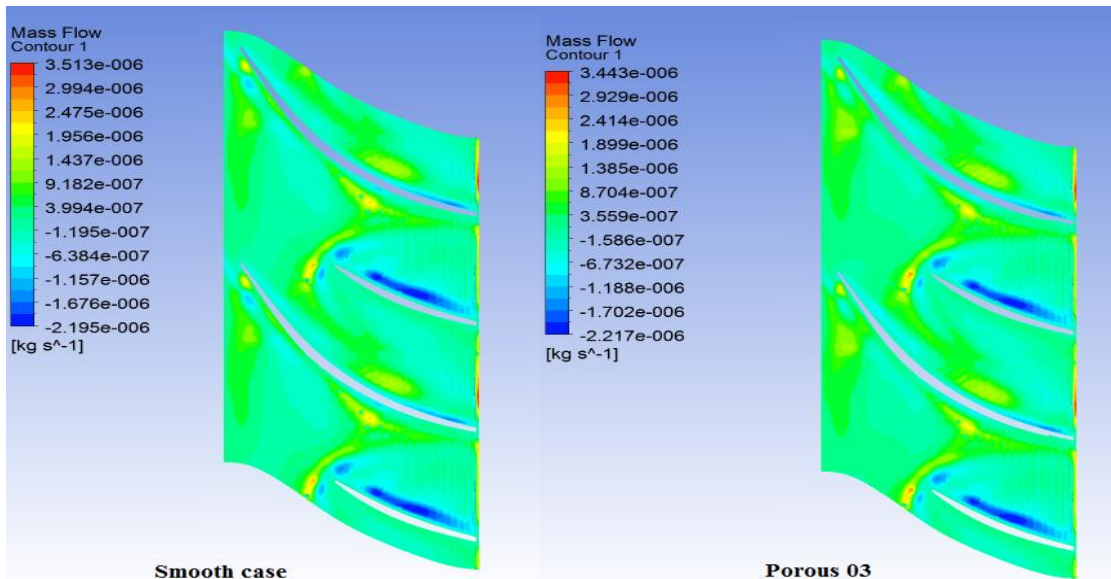


Fig.12: Mass Flow contours on a section located at 99 % of the impeller and diffuser spanwise direction for the smooth case and porous strip 03

In order to further investigate the effect of porous strip 03 on the impeller flow instability, velocity contours have been plotted. The plots are shown in Figure 12 dedicate that adding porous strip 03 close to the diffuser inlet affects the flow profile. In comparison with the smooth case, the porous strip 03 can be seen to reduce the magnitude of reverse flow of the impeller. Thus, this gives a sign about the improvement in the flow structure carried about by the addition of porous strip 03. However, the strip close to the outlet of impeller does not cause a significant effect on the flow reversal at the diffuser inlet as shown in Figure 13. Adding porous strip 03 close to the trailing edge of the impeller blade causes a reduction of the low total pressure region at impeller blade suction side when compared with the smooth case, also a pressure builds up can be noticed at the compressor outlet which is an indication of a stall margin improvement [6].

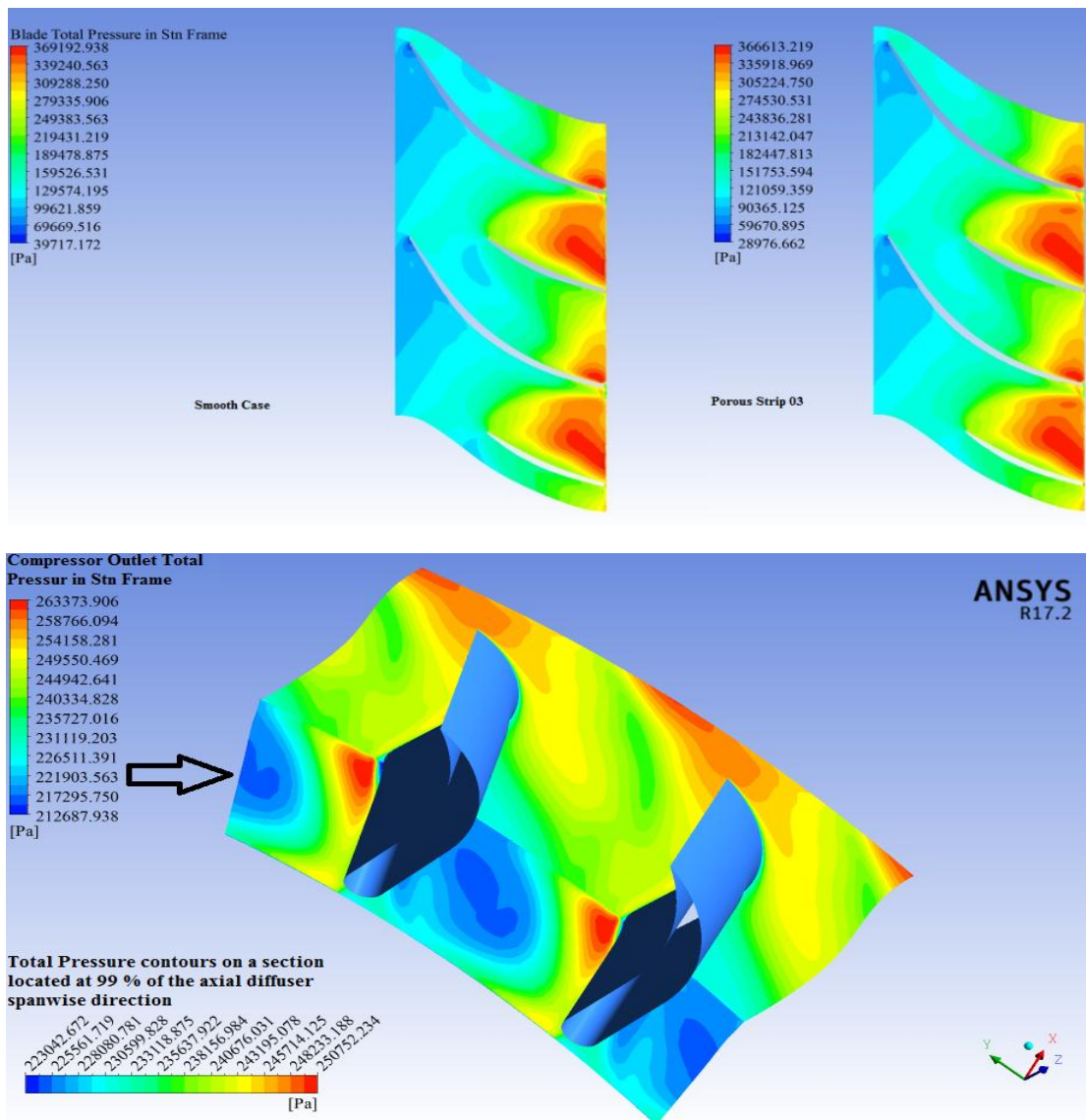


Fig.13: Total pressure contours on a section located at 99 % of the impeller and diffuser spanwise direction for the smooth case and porous strip 03

An improvement in velocity contours can be shown in Figure 14. The contour plots reveal a reduction in the wake region at the blade trailing edge and an improvement in the compressor outlet flow speed.

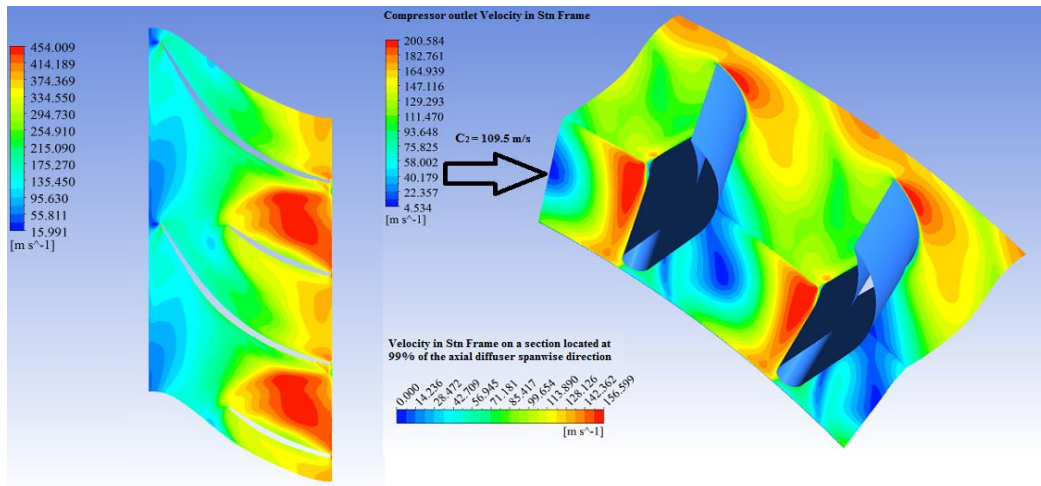
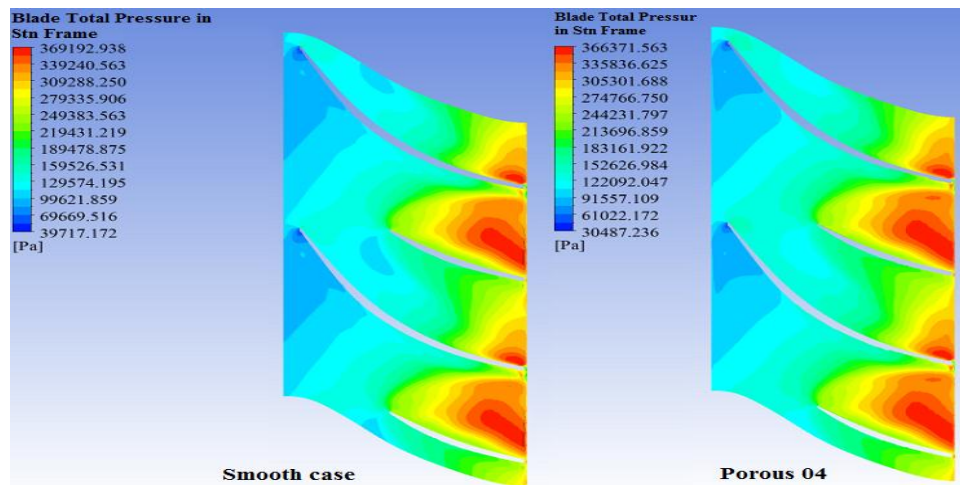


Fig.14: Velocity contours on a section located at 99 % of the impeller and diffuser spanwise direction for porous strip 03

2.4 Porous strip 04

Adding porous strip 04 has a similar effect to the results obtained by porous strip 03 where a reduction of the low total pressure region at the suction side of the impeller blade is noticed when compared with smooth case. Also a noticeable pressure builds at the compressor outlet which is an indication of a stall margin improvement [7] as shown in Figure 15.



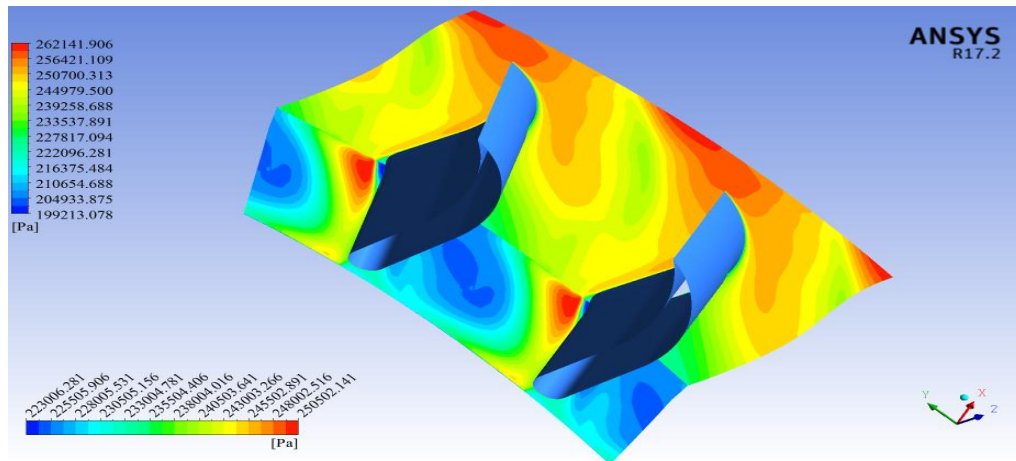


Fig.15: Total pressure contours on a section located at 99 % of the impeller and diffuser spanwise direction for the smooth case and porous strip 04

Figure 16 dedicates that adding porous strip 04 to the impeller results in reducing the distribution of the mass flow at the impeller in comparison with the porous strip 01 and strip 02 in the impeller domain.

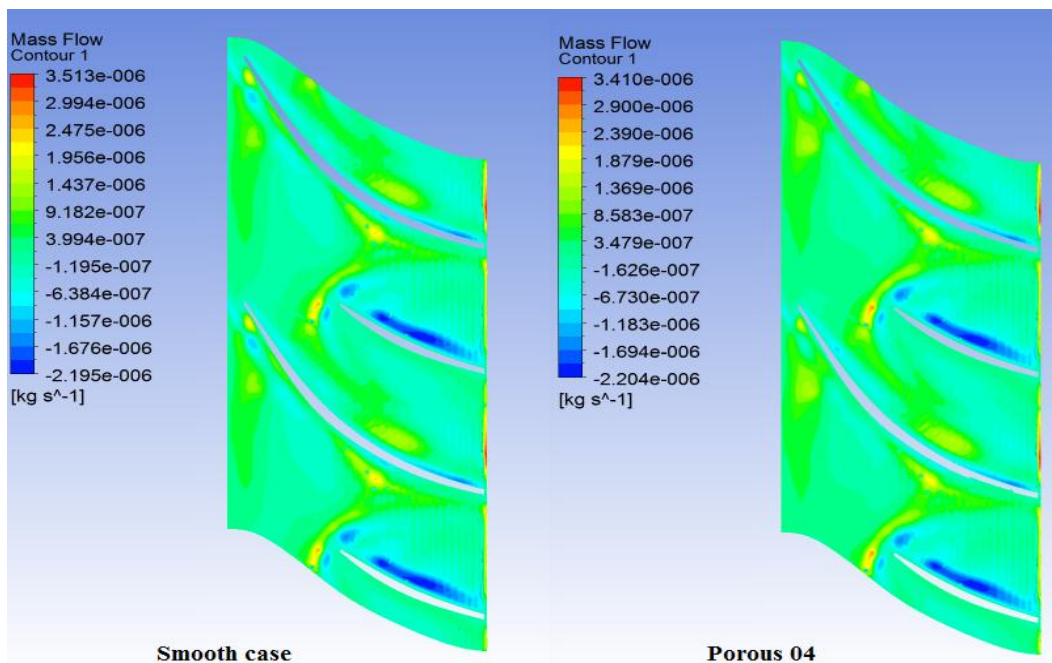


Fig.16: Mass Flow contours on a section located at 99 % of the impeller and diffuser spanwise direction for the smooth case and porous strip 04

Figure 17 shows improvement in velocity contours due to the addition of porous strip 04. The contour plots reveal an improvement in the compressor outlet flow speed.

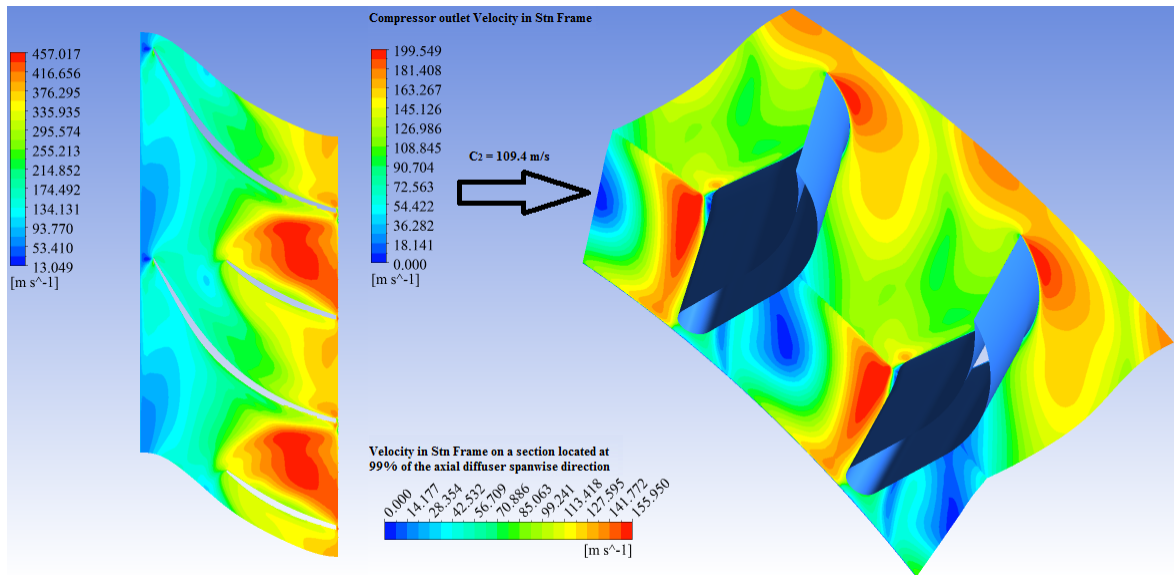
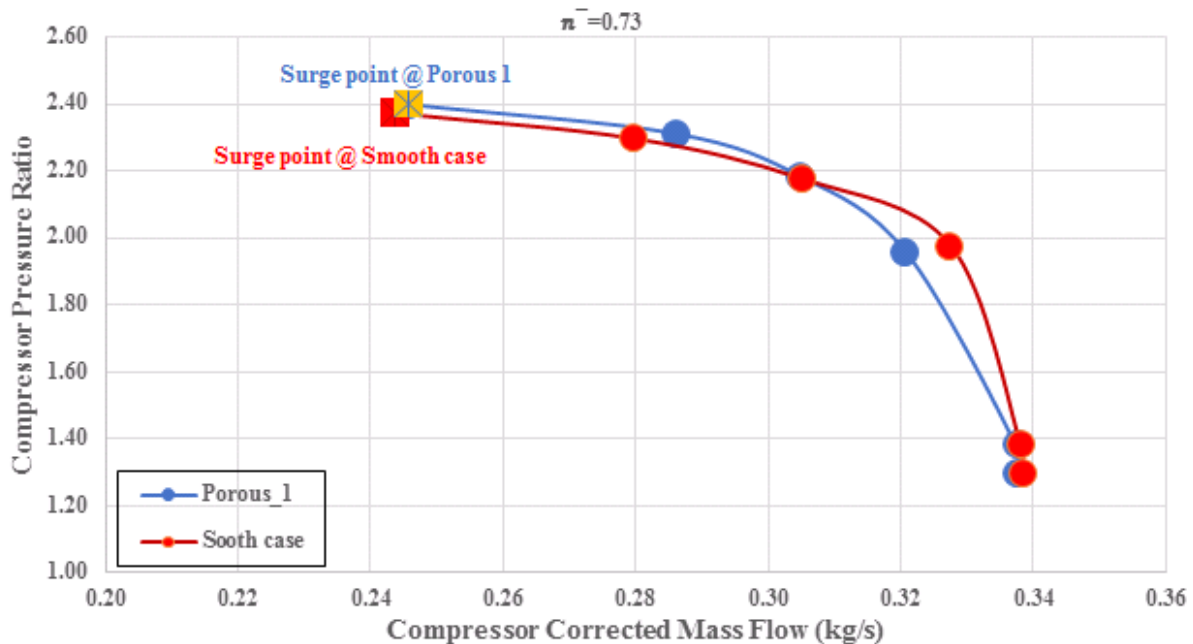


Fig.17: Velocity contours on a section located at 99 % of the impeller and diffuser spanwise direction for porous strip 04

3. Performance for test cases

Figure 18 to Figure 21 show the compressor performance curves of two test cases for $\bar{n} = 0.73$ & $\bar{n} = 0.85$ in order to compare each with the reference case and to compute the effect of adding the porous strips.



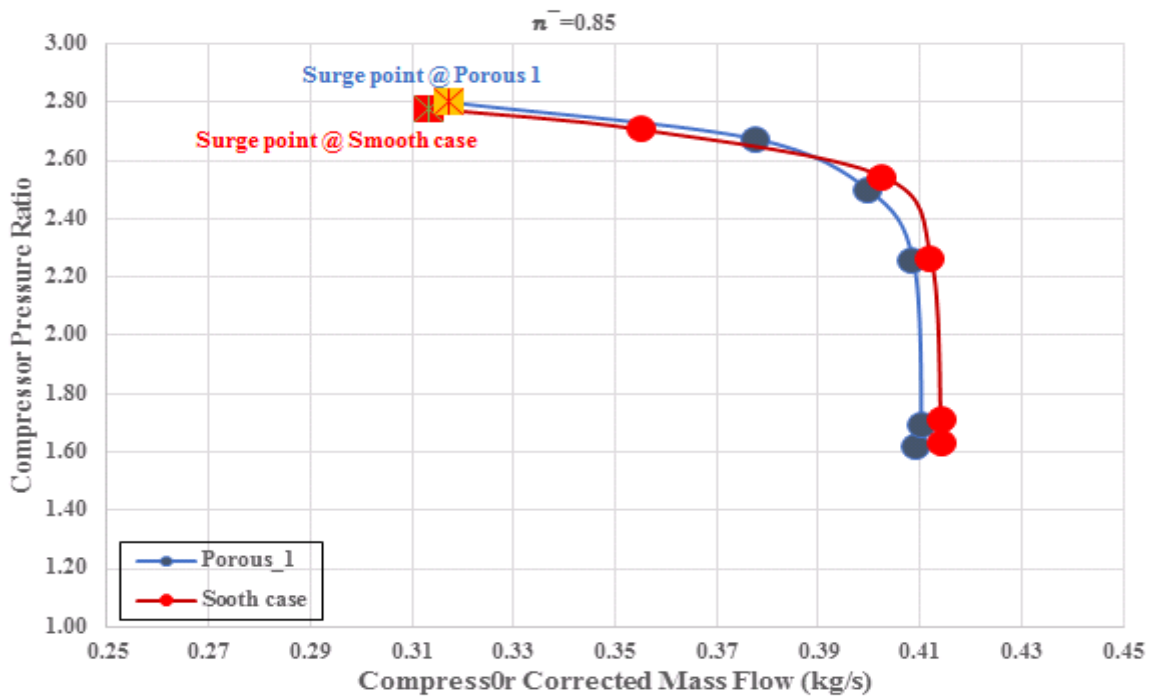


Fig.18: Comparing pressure ratio vs. /corrected mass flow at the smooth case and porous strip 01 for $\bar{\eta} = 0.73 \& 0.85$

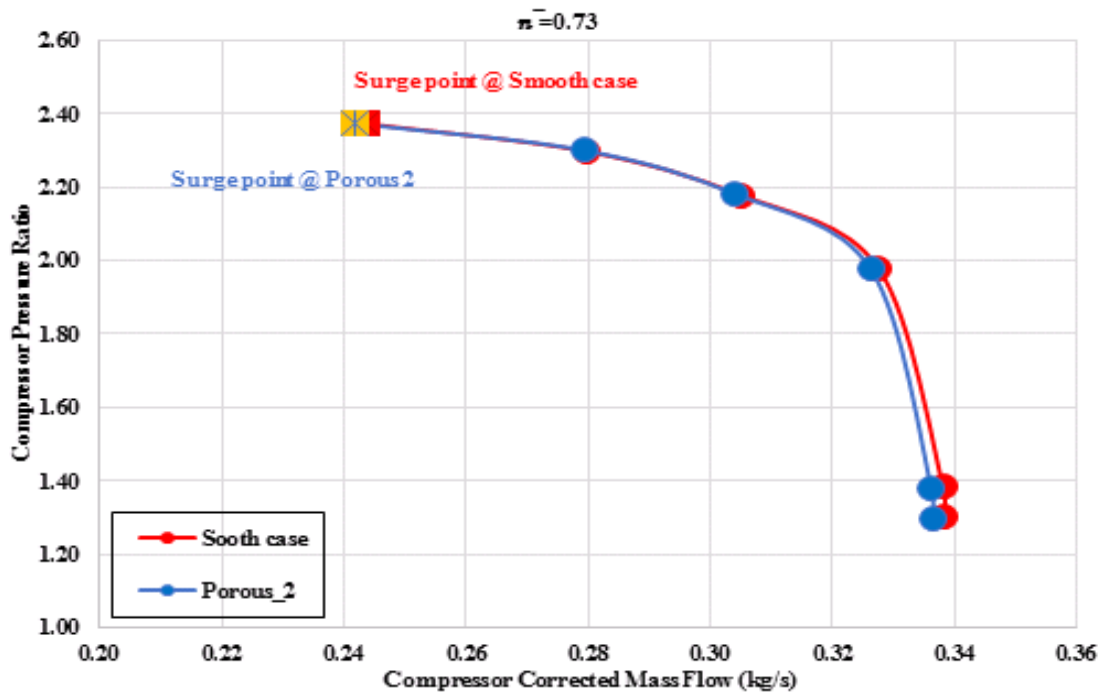


Fig.19: Comparing pressure ratio vs. /corrected mass flow at the smooth case and porous strip02 for $\bar{\eta} = 0.73 \& 0.85$

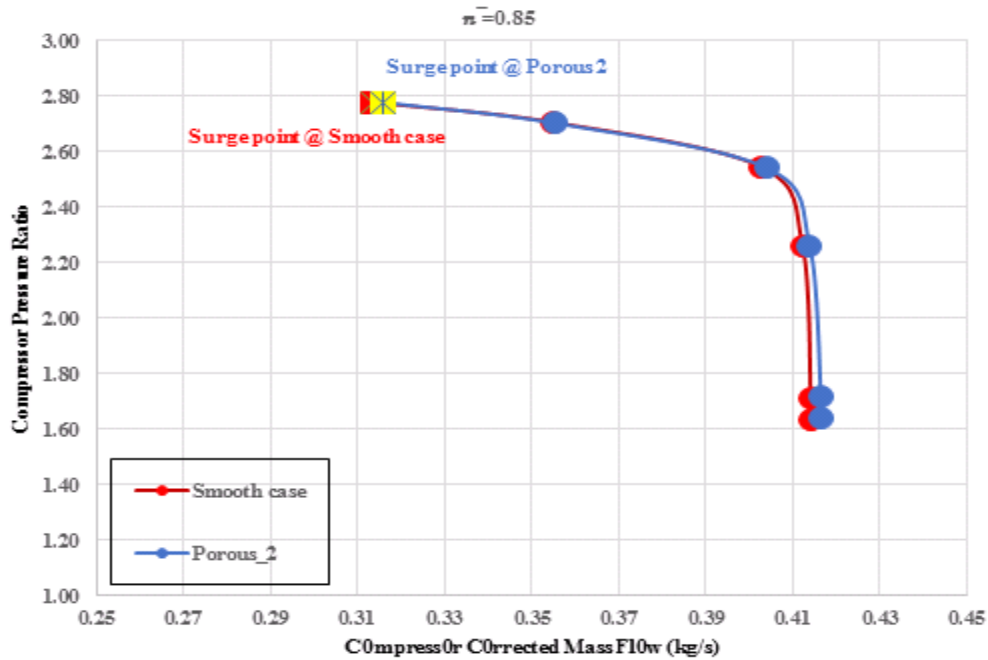


Fig.20: Comparing pressure ratio vs. /corrected mass flow at the smooth case and porous strip 03 for $\bar{n} = 0.73$ & 0.85

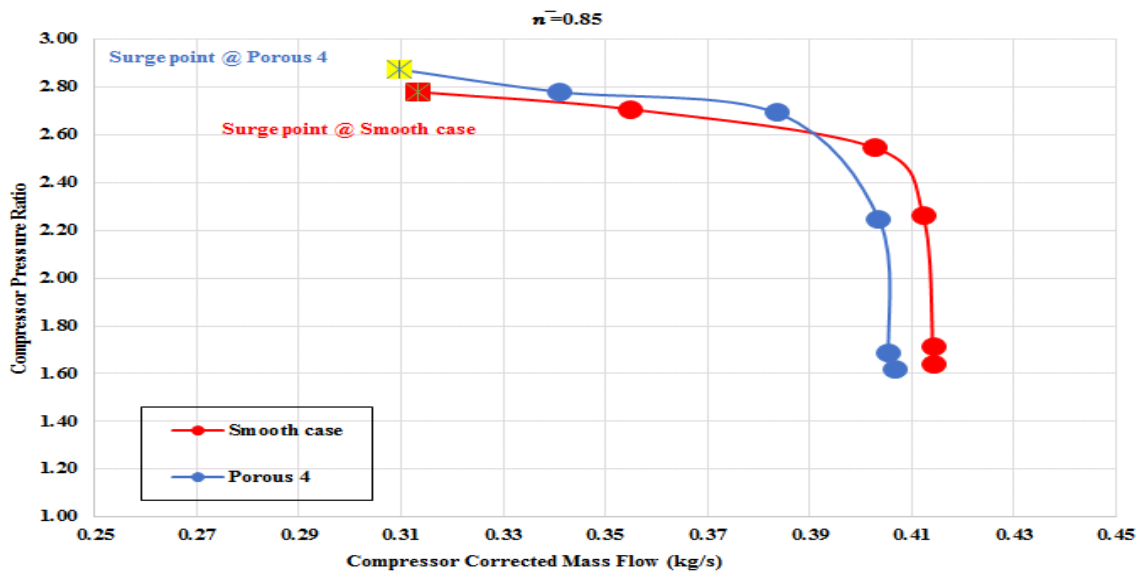


Fig.21: Comparing pressure ratio vs. /corrected mass flow at the smooth case and porous case 04 for $\bar{n} = 0.73$ & 0.85

It can be conducted from the previous figures that the porous strip 01, 03 and 04 on the suction side of impeller blades provides a stall margin improvement with no penalty for the total pressure ratio over the entire operating range when compared with the reference smooth case. However, the performance curves of the compressor with porous strip 02 are always identical with the reference case. The porous strip 02 is ineffective with regard to the increase of the stable operating range relative to the reference case. Also, by comparing the results obtained from adding the porous strip, it can be revealed that the porous strips 03 & 04 have a higher improvement effect on the compressor performance and the stall margin [8]. An additional attempt has been carried out to discuss this phenomenon by running simulation using porous strip 03 and strip 04

cases to evaluate the compressor map to compare it with the reference case. The underlying flow phenomena should be resolved by a more detail flow analysis using the simulation results.

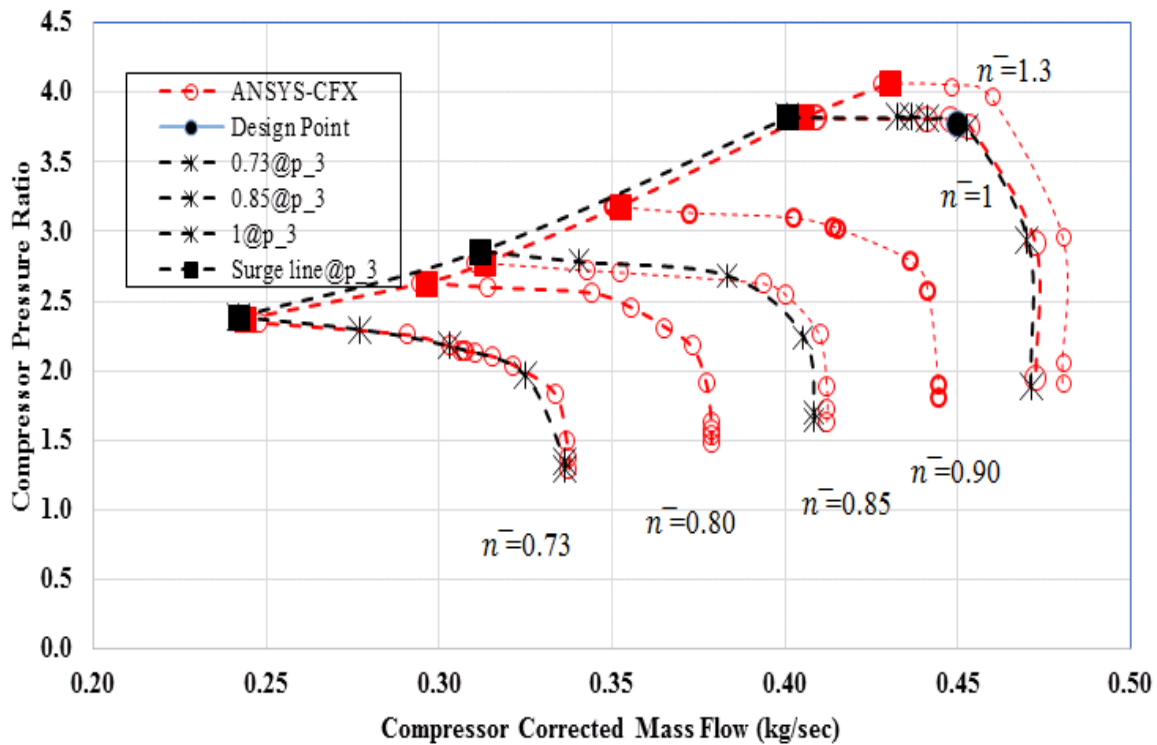


Fig.22: Comparing pressure ratio vs. /corrected mass flow at the smooth case and porous strip 03

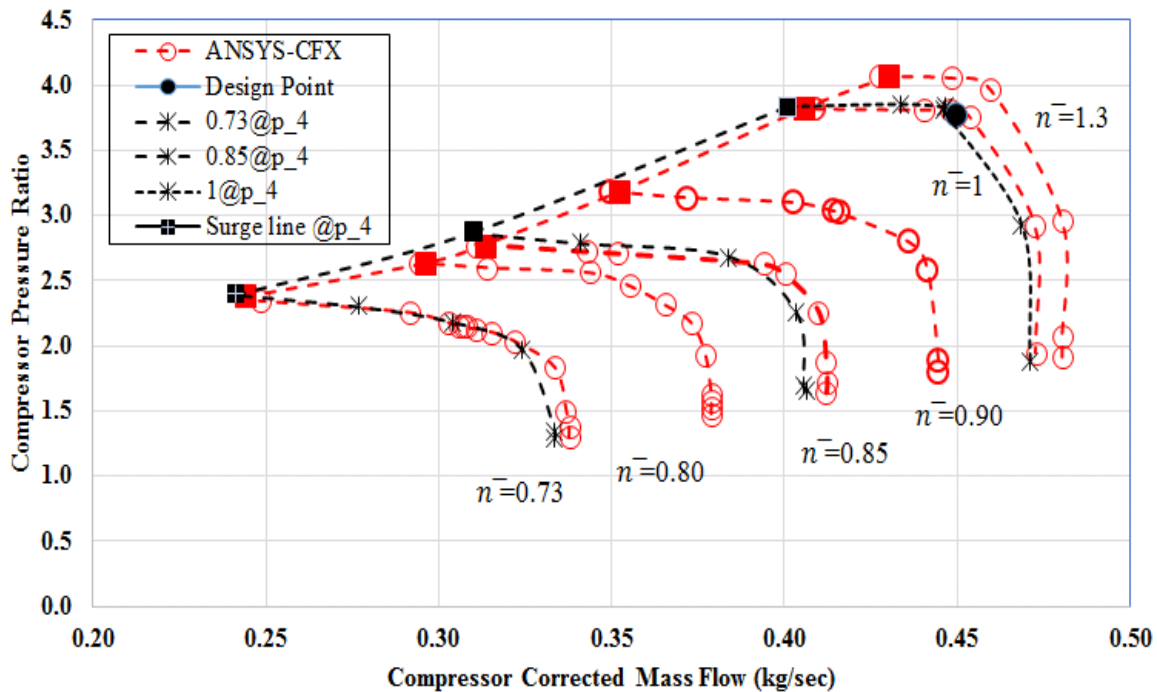


Fig.23: Comparing pressure ratio vs. /corrected mass flow at the smooth case and porous strip 04

4. Conclusions

A parametric study for using porous material strips at different positions of impeller blades suction side was performed to investigate their effect on the flow instabilities of the centrifugal compressor. Adding porous strips causes a reduction in the low momentum wake regions along the impeller blade. In addition to this, it also causes an improvement in the mass flow distribution close to the trailing edge.

Addition of the porous strip close to the impeller blades leading edge results in the reduction of low momentum region. The analysis reveals that the addition of porous strip close to the blade trailing edge results in an improvement in the flow structure, which leads to increase of the compressor surge margin by 9.2%.

5. NOMENCLATURE

Symbol	Description
π_{ct}	Compressor pressure ratio
F	Maximum Thrust
\dot{m}	Mass Flow Rate
EGT	Exhaust Gas Temperature
\bar{n}	Relative velocity
η_{ct}	Isentropic total efficiency of the compressor

6. REFERENCES

- [1]T. S. Fathy, et al., "Micro TJE centrifugal compressor performance prediction Tamer S," Journal of Engineering Science and Military Technologies, vol. 2, pp. 185-203, 2018.
- [2]X. Wang and X. Zhong, "Effect of porous coating on boundary-layer instability," in 48th AIAA Aerospace Sciences Meeting Including the New Horizons Forum and Aerospace Exposition, 2010, p. 1243.
- [3]M. Choi, et al., "Effects of the Inlet Boundary Layer Thickness on Rotating Stall in an Axial Compressor," in Turbo Expo: Power for Land, Sea, and Air, 2008, pp. 497-507.
- [4]M. Arai and T. Suidzu, "Porous ceramic coating for transpiration cooling of gas turbine blade," Journal of Thermal Spray Technology, vol. 22, pp. 690-698, 2013.
- [5]S. A. S. Ali, et al., "BOUNDARY LAYER FLOW INTERACTION WITH POROUS SURFACES."
- [6]X. Liu, et al., "Aerodynamic and aeroacoustic performance of serrated airfoils," in 21st AIAA/CEAS Aeroacoustics Conference, 2015, p. 2201.
- [7]S. L. Dixon and C. Hall, Fluid mechanics and thermodynamics of turbomachinery: Butterworth-Heinemann, 2013.
- [8]H. Saravanamuttoo and G. Roger, "Cohen, Gas Turbine Theory," England+ Pearson Education Limited, pp. 1-20, 2001.